Nonlinear thermal response of a Lennard-Jones fluid near the triple point

G. V. Paolini, G. Ciccotti, and C. Massobrio
Dipartimento di Fisica, Università degli Studi di Roma "La Sapienza," piazzale Aldo Moro 2, I-00185 Roma, Italy
(Received 6 February 1986)

We have carried out some more nonlinear molecular-dynamics calculations of the conductivity of the Lennard-Jones fluid near its triple point as a function both of the number of particles and of the external field. We have employed the subtraction technique and Evans-Gillan algorithm together with a recently proposed criterion to compare the strengths of impulsive and stationary perturbations. Accordingly, the gradients we used lie in the range 1.2×10^{7} to 5.8×10^{9} K/cm. Our results suggest that the response of the energy current at $\mathbf{K}=\mathbf{0}$ is linear for $\tilde{F}$ up to 5.8×10^{8} K/cm. We find nonlinearity for larger values of the perturbation. No dependence of the response on the particle number is found.

I. INTRODUCTION

In this paper we report a nonequilibrium molecular-dynamics (NEMD) computation of the thermal response of a simple fluid near its triple point as a function both of the imposed perturbation and of the number of particles.

We simulate a set of thermal gradients by mechanical perturbations using the Evans-Gillan[1,2] translationally invariant algorithm and the subtraction technique. We perturb the system with an impulsive force of strength $\tilde{F}$.

In a previous paper[3] a similar calculation of the thermal response of fluid argon has been reported for perturbations ranging from 9.57×10^{-10} up to 3.2×10^{-3} (in Verlet's units). Linearity was found throughout the whole range.

The purpose of the present work is to investigate further all possible dependences of the response on the strength of the perturbation, using the same method and the same kind of perturbing field as in Ref. 3. We apply a set of perturbations covering almost 3 orders of magnitude, from 3.2×10^{-3} up to 1.6. Our lowest value of $\tilde{F}$ corresponds to the highest value used in Ref. 3, where almost 6 orders of magnitude had been spanned, beginning with very weak fields.

The linear region extended up to $\tilde{F}=1.6\times10^{-1}$. For higher values of the external field we obtain a nearly linear increase of the ratio between the response and the external perturbation as a function of $\tilde{F}$. On the other hand, we find no significant variation of this ratio due to a change in the particle number, for $\tilde{F}$ belonging to the linear region.

In Ref. 3 a numerical comparison between $\tilde{F}$ and real thermal gradients was made according to the formula $\tilde{F}/h=\bar{F}=|\nabla T|/T$, where $\bar{F}$ is the stationary Θ-like perturbation employed in Ref. 1 and h is the time step of the numerical integration ($h=10^{-14}$ sec). Due to this choice the linear region of Ref. 3 which resulted was much larger than in Ref. 1. It has been suggested[4] that the method used in Ref. 3 to compare field strengths corresponding to impulsive or stationary perturbations is not satisfactory. An exact way to make such a comparison does not exist but we will apply an approximate method which has been successfully tested to compute diffusion in a system of two hard disks.[4] According to the new criterion the range of $\tilde{F}$ values used in Ref. 3 and in the present work corresponds approximately to thermal gradients from 3.5 to 5.8×10^{9} K/cm, while Evans's range goes from 1.27×10^{8} to 1.52×10^{9} K/cm.

We use the same mechanical coupling as in Ref. 1 to simulate thermal gradients but there are several differences between Evans's calculations and ours.

The first one is the time dependence of the perturbation. In Ref. 1 the applied field is a step function, while we adopt an impulsive force. This is not crucial within the linear region, because according to the linear-response theory these two choices are mathematically equivalent apart from a trivial integration, while for nonlinear perturbations there are remarkable differences due to the fact that we can no longer obtain the stationary thermal response making a linear superposition of impulsive effects. This difference is not relevant because the mechanical perturbation simulates a thermal gradient only in the linear regime.

A second difference lies in the fact that the differential method uses the first dynamical part of each perturbed trajectory, while Evans begins to take his averages after the transient stage, when the response becomes stationary. The steady state is maintained by removing the heat produced in the system. This is achieved by rescaling the second moment of the velocity.

Since we use an impulsive force we do not need any thermostat for $\tilde{F}$ up to 1.6×10^{-1} ($\approx5.8\times10^{8}$ K/cm). For higher values of $\tilde{F}$ the variation of the internal energy is such that the perturbed system decays to a different temperature. However, this happens in the region that turns out to be the nonlinear one.

Between the results of Refs. 1 and 3 for the conductivity there was also a small numerical discrepancy. A possible reason for this discrepancy could have been the dependence of the response on the particle number and on the cutoff radius. Evans used a system with $N_P=108$ and $R_C=2.5\sigma$, while the values of Ref. 3 were $N_P=256$ and

$R_C=3.35\sigma$. In order to isolate all possible sources of differences we use a cutoff radius $R_C=2.5\sigma$ throughout our calculations, as in Ref. 1.

Our results suggest that the numerical discrepancy was essentially irrelevant, at most an effect of the linear extrapolation used in Ref. 1.

In the first part of our work we study the thermal response as a function of the number of particles, keeping the external field fixed and equal to 3.2×10^{-3}.

In the second part we set $N_P=108$ and vary the strength of the applied perturbation.

For $\tilde{F}$ in the linear region we obtained values of λ which are consistent with both Ref. 1 and Ref. 3. For $\tilde{F}$ greater than 0.16 ($\approx5.8\times10^8$ K/cm) we find a nonlinear behavior similar to that of Ref. 1. On the other hand, our results show no significant variation due to the change in the particle number.

In Sec. II we give a simplified version of Evans's extension of linear-response theory to treat thermal non-Hamiltonian perturbations with Hermitian propagators. Section III describes the differential method and estimates the time dependence of its statistical error. In Sec. IV we discuss the form of the mechanical perturbation. In Sec. V we describe the model used in our calculations and implement the method. Section VI presents our results.

II. NON-HAMILTONIAN LINEAR-RESPONSE THEORY

We consider a system of N_P particles with coordinates $q_1,q_2,\ldots,q_{N_P}$ and a momenta $p_1,p_2,\ldots,p_{N_P}$, subjected to an external time-dependent perturbation $F(t)$. Its equations of motion are

$$\dot{\mathbf{q}}_i=\frac{\partial H^0}{\partial \mathbf{p}_i}+\mathbf{F}(t)\cdot\overleftrightarrow{C}_i=\frac{\mathbf{p}_i}{m}+\mathbf{F}(t)\cdot\overleftrightarrow{C}_i\,, \tag{2.1}$$

$$\dot{\mathbf{p}}_i=-\frac{\partial H^0}{\partial \mathbf{q}_i}+\mathbf{F}(t)\cdot\overleftrightarrow{D}_i=\mathbf{F}_i+\mathbf{F}(t)\cdot\overleftrightarrow{D}_i\,, \tag{2.2}$$

where $H^0=H^0(\{q_j,p_j\}_{j=1}^{j=N_P})$ is the Hamiltonian in the absence of $\mathbf{F}(t)$ and $\overleftrightarrow{C}_i=\overleftrightarrow{C}_i(\{q_j,p_j\}_{j=1}^{j=N_P})$ and $\overleftrightarrow{D}_i=\overleftrightarrow{D}_i(\{q_j,p_j\}_{j=1}^{j=N_P})$ are tensors of suitable nature. Equations (2.1) and (2.2) are not necessarily derivable from a Hamiltonian. In the thermal case *ad hoc* forms for $\overleftrightarrow{C}_i$ and $\overleftrightarrow{D}_i$ (Refs. 1 and 2) are

$$\overleftrightarrow{C}_i=\overleftrightarrow{0}, \tag{2.3}$$

$$\overleftrightarrow{D}_i=\left[E_i-\frac{1}{N_p}\sum_l E_l\right]\overleftrightarrow{1}+\frac{1}{2}\left[\sum_{j(\neq i)}\mathbf{F}_{ij}\mathbf{q}_{ij}-\frac{1}{N_P}\sum_j\sum_{k(\neq j)}\mathbf{F}_{jk}\mathbf{q}_{jk}\right], \tag{2.4}$$

where E_i, the total energy of particle i, $\mathbf{F}_{ij}$, the mutual force, and $\mathbf{q}_{ij}$, the relative position of particles i and j, are given by

$$\mathbf{q}_{ij}=\mathbf{q}_i-\mathbf{q}_j,\quad q_{ij}=|\,\mathbf{q}_{ij}\,|\,,$$

$$E_i=\frac{p_i^2}{2m}+\tfrac{1}{2}\sum_{j(\neq i)}\Phi(q_{ij})\,,$$

$$\mathbf{F}_{ij}=-\frac{\partial\Phi(q_{ij})}{\partial q_{ij}}\frac{\mathbf{q}_{ij}}{q_{ij}}\,.$$

The resulting equations of motion are consistent with periodic boundary conditions and preserve total momentum. If it is zero at $t=0$ then, for any t, $\mathbf{P}(t)=\sum_i\mathbf{p}_i(t)=\mathbf{0}$.

Let us now define the perturbed operator associated with the Liouville equation as

$$-iL\,(t)f=\sum_i\left[\frac{\partial f}{\partial\mathbf{q}_i}\cdot\dot{\mathbf{q}}_i+\frac{\partial f}{\partial\mathbf{q}_i}\cdot\dot{\mathbf{p}}_i\right]+f\sum_i\left[\frac{\partial}{\partial\mathbf{q}_i}\cdot\dot{\mathbf{q}}_i+\frac{\partial}{\partial\mathbf{p}_i}\cdot\dot{\mathbf{p}}_i\right], \tag{2.5}$$

where f is the phase-space distribution function.

We note that with our choice of $\overleftrightarrow{C}_i$ and $\overleftrightarrow{D}_i$, and with the prescription $\mathbf{P}=\sum_i\mathbf{p}_i(t)=\mathbf{0}$, we have

$$\sum_i\left[\frac{\partial}{\partial\mathbf{q}_i}\cdot\dot{\mathbf{q}}_i+\frac{\partial}{\partial\mathbf{p}_i}\cdot\dot{\mathbf{p}}_i\right]=\mathbf{F}(t)\cdot\sum_i\left[\frac{\partial}{\partial\mathbf{q}_i}\cdot\overleftrightarrow{C}_i+\frac{\partial}{\partial\mathbf{p}_i}\cdot\overleftrightarrow{D}_i\right]=0\,. \tag{2.6}$$

Thus in the thermal case $iL\,(t)$ is a Hermitian operator and we can apply linear-response theory in its standard form. We find

$$\Delta f\,(t)=\beta f^0\int_0^t dt'\,e^{-iL^0(t-t')}\times\sum_i\left[\frac{\partial H^0}{\partial\mathbf{q}_i}\cdot\overleftrightarrow{C}_i\cdot\mathbf{F}(t')+\frac{\partial H^0}{\partial\mathbf{p}_i}\cdot\overleftrightarrow{D}_i\cdot\mathbf{F}(t')\right], \tag{2.7}$$

where iL^0 is the unperturbed Liouville operator and f^0 is the equilibrium probability distribution which was chosen as the initial condition [$f(0)=f^0$]. In Eq. (2.7) we have assumed that $\mathbf{F}(t)=\mathbf{0}$ for $t\leq0$.

The zero-wave-vector energy current density $\mathbf{J}^E(\mathbf{k}=\mathbf{0})$ is

$$\mathbf{J}^E(\mathbf{k}=\mathbf{0})=\frac{1}{V}\left[\sum_i\frac{\mathbf{p}_i}{m}E_i+\tfrac{1}{2}\sum_i\sum_{j(\neq i)}\left[\frac{\mathbf{p}_i}{m}\cdot\mathbf{F}_{ij}\right]\mathbf{q}_{ij}\right]. \tag{2.8}$$

Inserting (2.3) and (2.4) into (2.7) and taking into account Eq. (2.8) we have

$$\Delta f\,(t)=\beta Vf^0\int_0^t e^{-iL^0(t-t')}\mathbf{J}^E(\mathbf{k}=\mathbf{0})\cdot\mathbf{F}(t')dt'\,. \tag{2.9}$$

Given a dynamical variable $\mathbf{O}=\mathbf{O}(\{q_j,p_j\}_{j=1}^{j=N_P})$, with $\mathbf{O}(t)=e^{iL^0(t)}\mathbf{O}$, we find for the linear response

$$\langle\mathbf{O}\rangle_t=\langle\mathbf{O}\rangle_0+\beta V\int_0^t\langle\mathbf{O}(t-t')\mathbf{J}^E(\mathbf{k}=\mathbf{0})\rangle_0\cdot\mathbf{F}(t')dt'\,. \tag{2.10}$$

Choosing $\mathbf{O}=\mathbf{J}^E(\mathbf{k}=\mathbf{0})$ Eq. (2.10) becomes

$$\langle\mathbf{J}^E(\mathbf{k}=\mathbf{0})\rangle_t=\beta V\int_0^t\langle\mathbf{J}^E(\mathbf{k}=\mathbf{0},t-t')\mathbf{J}^E(\mathbf{k}=\mathbf{0})\rangle_0\cdot\mathbf{F}(t')dt' \tag{2.11}$$

which gives the linear response in energy current to the perturbation imposed to the system by Eqs. (2.1) and (2.2).

III. THE SUBTRACTION TECHNIQUE

In this section we review the subtraction technique.[5] The evolution of a dynamical variable $\mathbf{O}$ subjected to a general perturbation which can be non-Hamiltonian can be written as

$$\mathbf{O}(t)=U(t)\mathbf{O},$$

where $U(t)=U(t,0)$ is the evolution operator from 0 to t. The corresponding time evolution of the probability density is

$$f(t)=U^{\dagger}(t)f^{0},$$

where $U^{\dagger}$ is the adjoint of U, even when U is not a unitary operator.[6]

Like in the Hamiltonian case we can exploit the equivalence between the Schrödinger and the Heisenberg pictures obtaining, for the nonequilibrium average of an observable $\mathbf{O}$, the form

$$\begin{aligned}\langle \mathbf{O}\rangle_t &\equiv (\mathbf{O},f(t))=(\mathbf{O},U^{\dagger}(t)f^{0})\\ &=(U(t)\mathbf{O},f^{0})=(\mathbf{O}(t),f^{0})\equiv\langle \mathbf{O}(t)\rangle_0,\end{aligned} \tag{3.1}$$

where $\langle\cdots\rangle_t$ denotes an ensemble average over $f(t)$, $\langle\cdots\rangle_0$ over f^0 and $(\cdots,\cdots)$ a scalar product, i.e., the integral over phase space. The meaning of Eq. (3.1) is that we can express the nonequilibrium average of the observable as the equilibrium average of the observable time evolved under the perturbed dynamics.

In the present case

$$\sum_i\left[\frac{\partial}{\partial \mathbf{q}_i}\cdot\dot{\mathbf{q}}_i+\frac{\partial}{\partial \mathbf{p}_i}\cdot\dot{\mathbf{p}}_i\right]=0 .$$

Therefore the probability density evolves like a $6N_P$-dimensional incompressible fluid and $U(t)$ is a unitary operator. From now on we will indicate with $U^0(t)$ the time evolution of $\mathbf{O}$ at equilibrium and with $U(t)$ the perturbed evolution.

Let us consider the case in which the equilibrium average of the observable is zero,

$$\langle \mathbf{O}\rangle_0\equiv\langle U^0(t)\mathbf{O}\rangle_0=0 . \tag{3.1'}$$

We can obtain the response in $\mathbf{O}$, at a time t since the switching on of the perturbation, by computing the quantity

$$\Delta\mathbf{O}(t)=U(t)\mathbf{O}-U^0(t)\mathbf{O} \tag{3.2}$$

and averaging it over an equilibrium ensemble. Indeed, making use of Eqs. (3.1) and (3.1'),

$$\begin{aligned}\langle \mathbf{O}\rangle_t=\langle \mathbf{O}\rangle_t-\langle \mathbf{O}\rangle_0&=\langle U(t)\mathbf{O}\rangle_0-\langle U^0(t)\mathbf{O}\rangle_0\\ &=\langle\Delta\mathbf{O}(t)\rangle_0 .\end{aligned} \tag{3.3}$$

The advantage of computing $\Delta\mathbf{O}(t)$ lies in the fact that the statistical noise can be reduced by several orders of magnitude as long as the perturbed and unperturbed trajectories are strongly correlated. To see this we can analyze the variance of the observable. It is given by

$$\begin{aligned}v[U(t)\mathbf{O}-U^0(t)\mathbf{O}]=&v[U(t)\mathbf{O}]+v[U^0(t)\mathbf{O}]\\ &-2\,\mathrm{cov}[U(t)\mathbf{O},U^0(t)\mathbf{O}] .\end{aligned} \tag{3.4}$$

In Eq. (3.4) the two variance terms on the right-hand side (rhs) have almost the same value while for a certain time the covariance term can be approximated with the square root of the product of the two variances. Under these conditions it can be easily shown that the variance of the difference is of the order of the perturbation square. When the covariance starts to decay to zero the noise increases. A rough test of the decay law of the covariance indicates an exponential decay with a characteristic time slightly larger than the decay time of energy current.

Let τ_C be the correlation time of the observable over the two trajectories. The subtraction is successful in the study of processes involving times not much longer than τ_C and for correlations decaying faster than polynomials. For example, in the case at hand the decay time of the energy autocorrelation function $C_E(t)$, defined as

$$\tau_E=\int_0^{\infty}C_E(t)dt ,$$

is about 20–25 time steps, smaller than τ_C and largely within the precision of the subtraction technique. A detailed study of the range and precision of the subtraction technique will be published elsewhere.[7]

IV. FORM OF THE PERTURBATION

The thermal conductivity is defined as[8]

$$\begin{aligned}\lambda&=\frac{V}{3k_BT^2}\int_0^{\infty}\langle \mathbf{J}^E(\mathbf{k}=0,t)\mathbf{J}^E(\mathbf{k}=0,0)\rangle_0 dt\\ &=\frac{\langle \mathbf{J}^{E^2}(\mathbf{k}=0)\rangle_0 V}{3k_BT^2}\int_0^{\infty}C_E(t)dt ,\end{aligned} \tag{4.1}$$

where

$$C_E(t)=\frac{\langle \mathbf{J}^E(\mathbf{k}=0,t)\mathbf{J}^E(\mathbf{k}=0,0)\rangle_0}{\langle \mathbf{J}^{E^2}(\mathbf{k}=0)\rangle_0}$$

and V and T are, respectively, the volume and the temperature of the system. Choosing

$$\mathbf{F}(t)=(0,0,\bar{F})\Theta(t) , \tag{4.2}$$

where

$$\Theta(t)=\begin{cases}0, & t<0\\ 1, & t\geq 0\end{cases}$$

and inserting (4.2) into (2.11) we find

$$\lambda=\lim_{t\to\infty}\left[\frac{\langle J_z^E(\mathbf{k}=0)\rangle_t}{\bar{F}T}\right] . \tag{4.3}$$

Another possible choice of the perturbation is

$$\mathbf{F}(t)=(0,0,\tilde{F})\delta(t) . \tag{4.4}$$

Substituting (4.4) in (2.11) we find

$$\langle J_z^E(\mathbf{k}=0)\rangle_t=\beta V\tilde{F}\langle \mathbf{J}_z^E(\mathbf{k}=0,t)\mathbf{J}_z^E(\mathbf{k}=0,0)\rangle_0 \tag{4.5}$$

and

$$\lambda=\frac{1}{\tilde{F}T}\int_0^\infty \langle J_z^E(\mathbf{k}=0)\rangle_t\,dt$$
$$=\frac{\langle J_z^E(\mathbf{k}=0)\rangle_{t=0}}{\tilde{F}T}\int_0^\infty \frac{\langle J_z^E(\mathbf{k}=0)\rangle_t}{\langle J_z^E(\mathbf{k}=0)\rangle_{t=0}}\,dt\ . \quad (4.6)$$

In Ref. 1 the first choice has been adopted. $\langle J_z^E(\mathbf{k}=0)\rangle_{t=\infty}$ is computed by averaging over the stationary part of the response, while the transient stage is disregarded. The system is maintained in the stationary state subtracting the heat produced by a suitable rescaling of the second moment of the velocity.

The choice of a Θ perturbation is possible with the subtraction technique too, even though it would prove more noisy. Therefore, in our calculations we preferred to adopt the impulsive form. The average is carried out along the equilibrium trajectory [Eq. (3.1)] thus obtaining the dynamical response.

These two choices of $\mathbf{F}(t)$ are equivalent only in the linear region. If $\mathbf{F}$ is given by (4.2) we obtain the complete response to the mechanical perturbation via (4.3) also in the nonlinear zone, while when adopting (4.4) and (4.6) we do not get all the necessary contributions because the response to a constant field is no longer obtained as a linear superposition of impulsive effects. However, the mechanical perturbation gives the thermal conductivity only in the linear region, therefore this difference is not relevant.

When we integrate the equations of motion we need to be careful at $t=0$ because in both cases a discontinuity arises:[5] with a Θ-like perturbation we have a change in acceleration due to the switching on of $\mathbf{F}(t)$, while when adopting an impulsive force we find a discontinuity in velocity.[3] The form of the discontinuity in our case is[3]

$$\mathbf{v}_i(0_+)-\mathbf{v}_i(0_-)$$
$$=\left[E_i-\frac{1}{N_P}\sum_l E_l\right]\overleftrightarrow{1}\cdot\frac{\tilde{\mathbf{F}}}{m}$$
$$+\frac{1}{2}\left[\sum_{j(\neq i)}\mathbf{F}_{ij}\mathbf{q}_{ij}-\frac{1}{N_p}\sum_j\sum_{k(\neq j)}\mathbf{F}_{jk}\mathbf{q}_{jk}\right]\cdot\frac{\tilde{\mathbf{F}}}{m}, \quad (4.7)$$

where the quantities depending on the velocity on the rhs are taken at $t=0_-$.

V. MODEL AND IMPLEMENTATION

The system of N_P particles is enclosed in a cube of side L, interacting through a Lennard-Jones potential

$$\Phi(r)=4\epsilon\left[\left(\frac{\sigma}{r}\right)^{12}-\left(\frac{\sigma}{r}\right)^{6}\right].$$

Our units are σ for length, ϵ for energy, and $\tau=(m\sigma^2/48\epsilon)^{1/2}$ for time.

We studied the thermal response of fluid argon ($\sigma=3.405$ Å, $\epsilon=119.8k_B$, $\tau=3.112\times10^{-13}$ sec) near its triple point ($N_P\sigma^3/V=0.8442$, $k_BT/\epsilon=0.721$) as a function of both the number of particles and the perturbation. Our boundary conditions are periodic in all directions.

To use the differential method[5] we perturb the system with an impulsive force at regular time intervals and simultaneously follow the particles' paths both in perturbed and unperturbed trajectories. We calculate the difference in the relevant dynamical variable on each pair of trajectories, then we average it over a number of such pairs. Thus we can observe the decay of the energy current as a function of t (the time elapsed since the switching on of the perturbation). With

$$\mathbf{F}(t)=\tilde{\mathbf{F}}\delta(t),$$

the equations of motion are

$$\dot{\mathbf{q}}_i=\frac{\mathbf{p}_i}{m}, \quad (5.1)$$

$$\dot{\mathbf{p}}_i=\sum_j\mathbf{F}_{ij}+\left[E_i-\frac{1}{N_p}\sum_j E_j\right]\overleftrightarrow{1}\cdot\tilde{\mathbf{F}}\delta(t)$$
$$+\frac{1}{2}\left[\sum_{j(\neq i)}\mathbf{F}_{ij}\mathbf{q}_{ij}-\frac{1}{N_P}\sum_{k(\neq j)}\mathbf{F}_{jk}\mathbf{q}_{jk}\right]\cdot\tilde{\mathbf{F}}\delta(t)\ . \quad (5.2)$$

These equations are integrated using the standard "leap-frog" algorithm, with a slight modification at $t=0$, because of the impulsive nature of $\mathbf{F}(t)$,[3] given by Eq. (4.7). Note that the $t=0$ algorithm is precise to $o(h^3)$.

Since we want to reproduce, as far as possible, the conditions of Ref. 1, we set $R_C=2.5\sigma$ and studied the dependence of the conductivity, at $N_P=108$ fixed, on the magnitude of the perturbation and at $\tilde{F}$ fixed as a function of N_P ($N_P=108$, 256, 500, and 864).

We computed the decay of the energy autocorrelation function by

$$C_E(t)=\frac{\langle J_z^E(\mathbf{k}=0)\rangle_t}{\langle J_z^E(\mathbf{k}=0)\rangle_{t=0}} \quad (5.3)$$

and the thermal conductivity by

$$\lambda=k_P\int_0^\infty C_E(t)dt\approx k_PI_W(t_P), \quad (5.4)$$

where

$$k_P=\frac{\langle J_z^E(\mathbf{k}=0)\rangle_{t=0}}{\tilde{F}T},$$

$I_W(t_P)$ is the weighted average of the integral

$$I(t)=\int_0^t C_E(t')dt'$$

over times $t_P\le t\le t_{\max}$, and t_P is the minimum time such that for $t\ge t_P$ $I(t)$ is stationary. The average $I_W(t_P)$ is weighted with the inverse of the variance of $I(t)$. This procedure has been used to reduce the uncertainty in the choice of the plateau value. This gives a more reliable estimate of the integral in Eq. (5.4).

VI. RESULTS

In this section we present the results of two series of calculations. In the first part of our work we studied the dependence of the thermal response on the particle num-

ber, at $\tilde{F}$ fixed and lying within the linear region. In the second part we investigated all possible variations of the response due to a change in the perturbation strength, at constant N_P.

The perturbations we used cover a wide range of values. Thus we were able to ascertain the extension of the linear region and to give an estimate of the numerical relationship betweeen the field strengths corresponding to impulsive and stationary perturbations more reliable than that provided in Ref. 3.

We estimated the error in λ by combining the two standard errors in k_P and in the integral $I_W(t_P)$ according to the formula

$$\frac{\Delta\lambda}{\lambda}=\left[\frac{\sigma^2(k_P)}{k_P^2}+\frac{\sigma^2(I_W)}{I_W^2}\right]^{1/2}. \tag{6.1}$$

The standard deviation on temperature is neglected. Since a rigorous statistical analysis of the error on the integral would be somewhat complicated, because the values of $I(t)$ are time correlated, we estimated it by the error on $I(t^*)$, where t^* is an intermediate time in the plateau region. We chose $t^*=110$ time steps equal to 3.52 in Verlet's units. As for $I(t^*)$, we estimated its error by considering the standard deviation of the variable

$$\tilde{I}(t^*)=\int_0^{t^*}\frac{J_z^E(\mathbf{k}=\mathbf{0},t)}{J_z^E(\mathbf{k}=\mathbf{0},0)}dt \tag{6.2}$$

on the assumption, supported by our results, that the correlation between the form of the relaxation and the value of $J_z^E(\mathbf{k}=\mathbf{0})$ at $t=0$ is negligible. Throughout our calculations we maintained the cutoff radius R_C equal to 2.5σ.

A. Dependence on N_P

In Fig. 1 we plot the results obtained by varying the number of particles. These results are reported in Table I. The value of the external field was held constant and equal to 3.2×10^{-3}.

We get better statistics when we increase the size of the system, $\mathbf{J}^E$ being an additive quantity [see Eq. (2.8)] with relative fluctuations going as $N_P^{-1/2}$ for large N_P. Thus, to save computer time, for different values of N_P the number of segments we compute decreases as the number of particles increases, in such a way to obtain comparable errors.

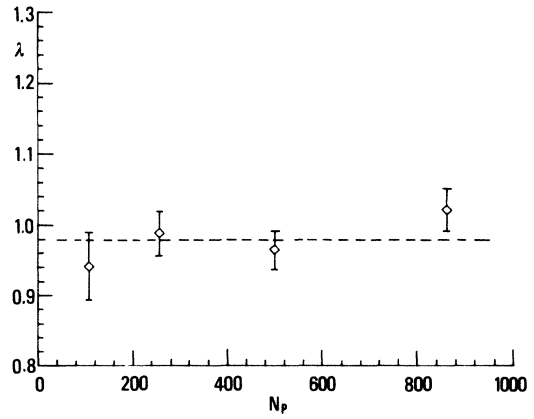

FIG. 1. Triple-point LJ conductivity as a function of the number of particles N_P. $\rho=0.8442$. The dashed line represents the average value (see text) $\bar{\lambda}=0.978\pm0.024$.

There is no apparent variation in the thermal conductivity on the increasing of the system size. From a linear least-squares fit through these results we have found an angular coefficient

$$b=8.41\times10^{-5}$$

with standard deviation

$$s(b)=4.1\times10^{-5}.$$

Thus, by applying standard statistical techniques we see that we have good consistency with the hypothesis of zero angular coefficient.

According to our analysis the most reliable value for λ is the average over the results for different numbers of particles

$$\bar{\lambda}=0.978\pm0.024.$$

B. Dependence on $\tilde{F}$

Figure 2 shows the results we obtained for the ratio of the thermal response and the external perturbation as a function of $\tilde{F}$ compared to some of the results of Ref. 1. In Table II we list the corresponding values for λ together with the values obtained in Ref. 3. We set $N_P=108$ throughout these calculations.

We employed perturbations from 3.2×10^{-3} up to 1.6. Our results show no dependence on $\tilde{F}$ for perturbations up

TABLE I. Results for thermal conductivity as a function of the number of particles N_P. T, temperature; N, total number of time steps; t_P is defined in Sec. V; k_P is defined in Sec. V; λ, thermal conductivity. $\tilde{F}=3.2\times10^{-3}$, $\rho=0.8442$, $R_C=2.5\sigma$. The last value of λ is the average of the previous four values (see text).

T (ϵ/k_B)	N_P	N		t_P	$k_P\pm\Delta k_P$ ($48\epsilon k_B/m\sigma^3$)	$\lambda\pm\Delta\lambda$ [$(k_B/\sigma)(48\epsilon/m\sigma^2)^{1/2}$]
0.721	108	15 000	(100×150)[a]	80	1.384±0.030	0.941±0.047
0.718	256	12 000	(80×150)	80	1.371±0.020	0.987±0.033
0.721	500	9000	(60×150)	80	1.387±0.018	0.963±0.027
0.719	864	4500	(30×150)	75	1.409±0.017	1.020±0.030
						0.978±0.024

[a]The first number in parentheses is the number of segments, the second the length of the segment.

to $\tilde{F}=0.16$ and are consistent with those obtained in Ref. 3, after a small correction. Indeed, the numerical integration of Eq. (5.4) was performed in Ref. 3 without considering that the value corresponding to $t=0$ has to be taken with a coefficient 0.5. From Fig. 2 we see that the first deviation from linearity appears between $\tilde{F}=1.6\times10^{-1}$ and 4.8×10^{-1}, and that the increase of the thermal response ratio is approximately linear.

According to the formula

$$\frac{\tilde{F}}{h}=\bar{F} \tag{6.3}$$

adopted by Massobrio and Ciccotti[3] to compare the strength of the impulsive force $\tilde{F}$ to that of the step function $\bar{F}$ the values from $\bar{F}=3.2\times10^{-3}$ to 4.8×10^{-2} were supposed to cover the entire range studied in Ref. 1.

Since we found a nonlinear behavior in our results corresponding to $\tilde{F}$ values somewhat larger than those expected according to (6.3) we looked for a new criterion for the comparison. If we consider the phenomenological law of thermal conduction

$$\mathbf{J}^E=-\lambda\nabla T$$

together with the relation $\bar{F}=|\nabla T|/T$ employed by Evans and formulas (4.3) and (4.6), we find that a good way to compare $\tilde{F}$ and $\bar{F}$ might be

$$\frac{\tilde{F}}{\tau}=\bar{F}, \tag{6.4}$$

where $\tau=\int_0^{t_P} C_E(t)dt\approx0.7$ (in Verlet's units) has the dimension of time and can be considered as a sort of decay time of the energy autocorrelation function. This procedure is the one suggested by Hoover *et al.* in Ref. 4, where a similar reasoning has been adopted to compute the diffusion of a system of two hard disks with both kinds of applied fields.

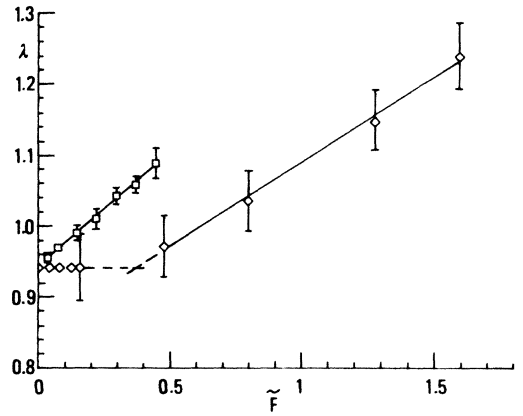

FIG. 2. Thermal conductivity as a function of the perturbation strength. □, data from Ref. 1; ◇, our results. $N_P=108$, $R_C=2.5\sigma$, $\rho=0.8442$. The two scales of the abscissas have been compared according to (6.4). The dashed lines extrapolate the linear and nonlinear data, respectively.

Employing (6.4) to compare our perturbations to those of Ref. 1 we find an extension of the scale on the abscissas by about a factor of 20 with respect to that of Ref. 3. This seems to be a reliable way of comparing $\tilde{F}$ to $\bar{F}$, even though it is not precise since it comes from an *a posteriori* estimate of τ.

From (6.4) we obtain

$$\bar{F}_{\min}\approx0.0046,\quad \nabla T_{\min}\approx1.2\times10^{7}\ \mathrm{K/cm},$$

$$\bar{F}_{\max}\approx2.29,\quad \nabla T_{\max}\approx5.8\times10^{9}\ \mathrm{K/cm}.$$

According to this estimate the $\bar{F}$ values of Ref. 1 lie

TABLE II. Results for the thermal conductivity as a function of the external field $\tilde{F}$. T, temperature; N, total number of time steps; k_P is defined in Sec. V; λ, thermal conductivity. $N_P=108$, $\rho=0.8442$, $R_C=2.5\sigma$. PCM, our results; MC, results of Ref. 3, corrected; EV, results of Ref. 1. $\tilde{F}$ is computed according to (6.4). $t_P=80$ for all $\tilde{F}$'s (t_P is defined in Sec. V).

T (ϵ/k_B)	$\tilde{F}$ $[(m/48\epsilon)^{1/2}]$	N		$k_P\pm\Delta k_P$ $(48\epsilon k_B/m\sigma^3)$	$\lambda\pm\Delta\lambda$ $[(k_B/\sigma)(48\epsilon/m\sigma^2)^{1/2}]$	Source
0.721	9.57×10^{-10} to 3.2×10^{-3}	10080	(84×120)	1.373±0.02	0.970±0.033	MC
0.721	3.2×10^{-3} to 8.0×10^{-2}	15000	(100×150)	1.384±0.030	0.941±0.047	PCM
0.721	1.28×10^{-1}	15000	(100×150)	1.385±0.030	0.941±0.047	PCM
0.721	1.6×10^{-1}	15000	(100×150)	1.386±0.030	0.941±0.047	PCM
0.721	4.8×10^{-1}	15000	(100×150)	1.404±0.031	0.972±0.043	PCM
0.721	8.0×10^{-1}	15000	(100×150)	1.443±0.034	1.035±0.042	PCM
0.721	1.28	15000	(100×150)	1.539±0.039	1.149±0.042	PCM
0.721	1.6	15000	(100×150)	1.627±0.045	1.239±0.047	PCM
0.722	3.5×10^{-2}	100000			0.955±0.007	EV
0.722	7.0×10^{-2}	48000			0.969±0.006	EV
0.723	1.4×10^{-1}	26000			0.99 ±0.01	EV
0.725	2.1×10^{-1}	35000			1.010±0.014	EV
0.727	2.8×10^{-1}	48000			1.042±0.012	EV
0.729	3.5×10^{-1}	39000			1.058±0.012	EV
0.729	4.2×10^{-1}				1.088±0.022	EV

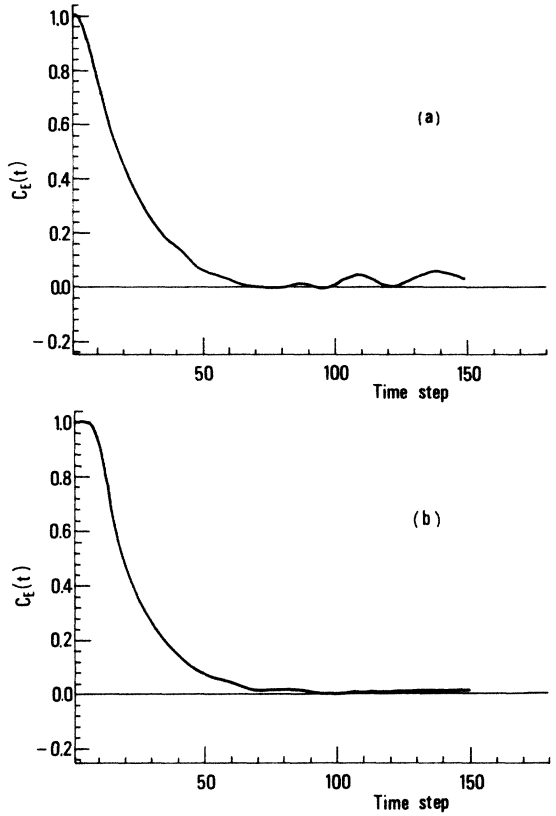

FIG. 3. $C_E(t)$. Normalized average relaxation of the energy current density. Average over 100 segments. (a) $\tilde{F}=0.16$, (b) $\tilde{F}=1.6$. $\rho=0.8442$.

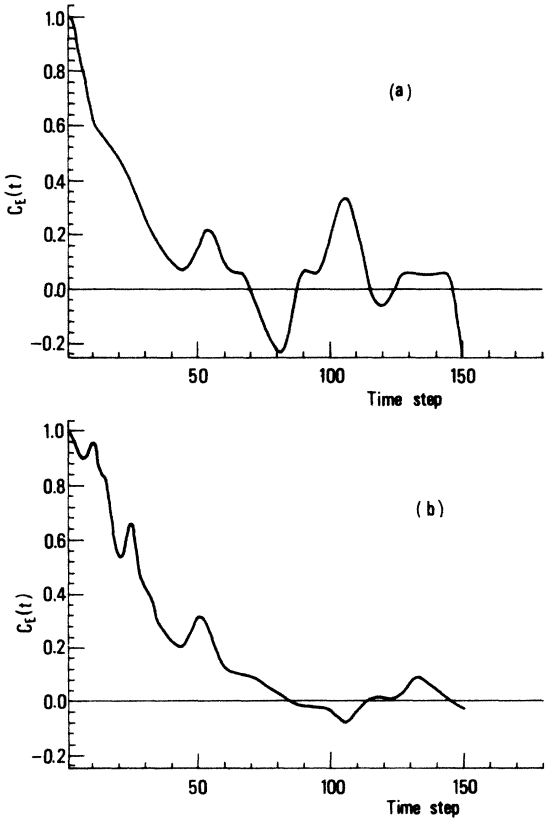

FIG. 4. Normalized relaxation of the energy current density for a single segment. (a) $\tilde{F}=0.16$, (b) $\tilde{F}=1.6$. $\rho=0.8442$.

within the range of the perturbations employed in the present work, as we show in Fig. 2.

We note that the slope of our nonlinear results is smaller than that found by Evans, in accordance with the fact that in the nonlinear region the integral of the autocorrelation function obtained with an impulsive field according to (4.6) contains less contributions than it should, for the reason mentioned in Sec. II.

In Fig. 3 we plot the average over 100 segments of the decay of the normalized energy current for two values of $\tilde{F}$: 0.16, still in the linear region, and 1.6, the highest value employed. We see in Fig. 3(b) that there is a sort of "plateau" near $t=0$ while for higher t the system decays toward the behavior of the linear case. An example of instantaneous decays of the energy current is plotted in Fig. 4, for linear and nonlinear cases, to clarify the decay mechanism in the nonlinear case. The two cases take approximately the same time for a complete decay, but the relaxation is altered in the nonlinear one, indicating that the system is unable to dissipate the "heat" induced by the external field in a single bunch. The integral of the normalized average relaxation of the energy current density is shown in Fig. 5.

The total energy too is altered in the nonlinear region. In Table III we report the total energy of the perturbed

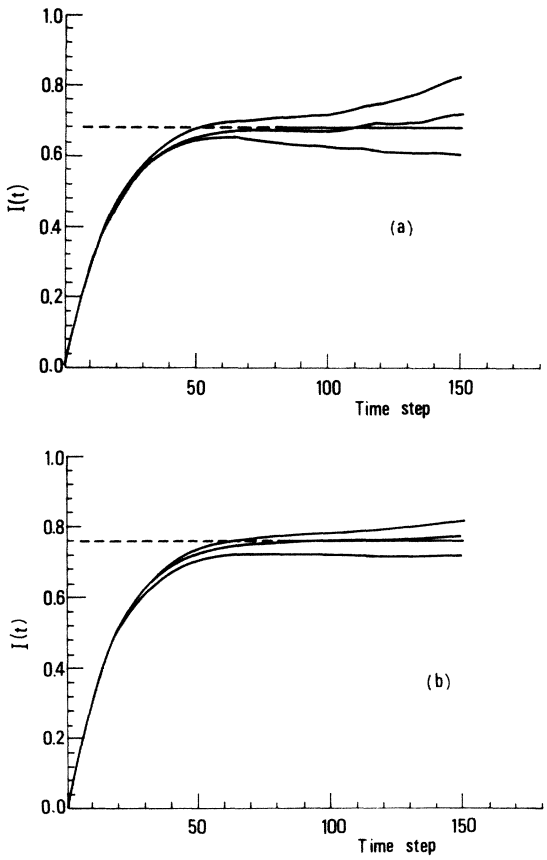

FIG. 5. $I(t)$. Integral of the normalized average relaxation of the energy current density. Straight line represents the value of the weighted average $I_W(t_P)$: the solid part delimits the set of points employed in the average (see text). (a) $\tilde{F}=0.16$, (b) $\tilde{F}=1.6$. $\rho=0.8442$.

TABLE III. Trend of the total energy in perturbed trajectories as a function of perturbation strength $\tilde{F}$. $\overline{E}_P$, total perturbed energy; $|\overline{\Delta E}|/E^0$, variation of the energy relative to the equilibrium average value; T_{est}, estimated value of the temperature of the corresponding microcanonical system at $\rho=0.85$ (interpolation from data of Ref. 9); $|\Delta T|/T^0$, variation of the temperature relative to the equilibrium average value. $\overline{E}^0=-5.013\,390$, $T^0=0.721$, $\rho=0.8442$.

$\tilde{F}$ $[(m/48\epsilon)^{1/2}]$	$\overline{E}_P$ (ϵ)	$\lvert\overline{\Delta E}\rvert/E^0$	T_{est} (ϵ/k_B)	$\lvert\Delta T\rvert/T^0$
3.2×10^{-3}	-5.013	7.7×10^{-7}	0.722	1.4×10^{-3}
4.8×10^{-2}	-5.012	2.4×10^{-4}	0.723	2.8×10^{-3}
8.0×10^{-2}	-5.010	7.0×10^{-4}	0.724	4.2×10^{-3}
1.28×10^{-1}	-5.004	1.8×10^{-3}	0.726	6.9×10^{-3}
0.16	-4.999	2.9×10^{-3}	0.728	9.7×10^{-3}
0.48	-4.880	2.7×10^{-2}	0.778	7.9×10^{-2}
0.80	-4.642	7.4×10^{-2}	0.879	2.2×10^{-1}
1.28	-4.059	1.9×10^{-1}	1.124	5.6×10^{-1}
1.6	-3.521	3.0×10^{-1}	1.350	8.7×10^{-1}

system as a function of the perturbation together with an estimate of the temperatures corresponding to these energies in a microcanonical ensemble. These values are obtained by linear interpolation from Verlet's data for the isochore at $\rho=0.85$.[9] We see that the variation of T is less than 1 K throughout the linear region, and becomes significant for $\tilde{F}$ larger than 0.16. For the largest perturbation employed the variation in $\overline{E}$ is of about 30% with respect to the equilibrium value, while the change in temperature is almost of 90%. This confirms the general idea that the onset of nonlinearity is associated with perturbations that alter the state of the system in a way which is significant up to the microscopic level.

VII. CONCLUSIONS

We have carried out some more NEMD computations of the conductivity of the LJ fluid near its triple point as a function both of the external field and of the number of particles. We employed the subtraction technique together with Evans-Gillan translationally invariant algorithm.[1,2]

We use a criterion recently suggested[4] to compare the field strengths of impulsive and stationary perturbations. This criterion has been applied to estimate the values of the thermal gradients corresponding to the δ-like mechanical perturbations used in the present work and in Ref. 3.

We extended the range of the perturbations used in Ref. 3 up to $\tilde{F}=1.6$ ($\approx5.8\times10^9$ K/cm) in order to find out the size of the linear region and to explain the nature of nonlinearity. We found linearity from $\tilde{F}=9.57\times10^{-10}$ to 1.6×10^{-1} (≈3.5 to 5.8×10^8 K/cm). The onset of nonlinearity occurs for $\tilde{F}$ around 4×10^{-1} ($\approx1.4\times10^9$ K/cm) and appears as a nearly linear increase of the ratio between the response and the external field. From Fig. 4(b) we see that this is an effect of the difficulty in dissipating the heat induced in the system by the external field. The time range of the decay is not very much altered in the nonlinear region. It is the speed of the relaxation that suffers a sensible slowing down.

The various homogenous NEMD algorithms have similar efficiency and reliability. However, we want to stress that the differential method, being a dynamical study of the response, can be particularly useful to show the mechanisms behind the onset of nonlinear effects.

ACKNOWLEDGMENTS

We are indebted to W. G. Hoover and J. P. Ryckaert for many useful discussions.

[1]D. J. Evans, Phys. Lett. **91A**, 457 (1982).
[2]M. Dixon and M. J. Gillan, J. Phys. C **16**, 869 (1973).
[3]C. Massobrio and G. Ciccotti, Phys. Rev. A **30**, 3191 (1984).
[4]W. G. Hoover, G. Ciccotti, G. V. Paolini, and C. Massobrio, Phys. Rev. A **32**, 3765 (1985).
[5]G. Ciccotti, G. Jacucci, and I. R. McDonald, J. Stat. Phys. **21**, 1 (1979).
[6]D. J. Evans, *Non-Equilibrium Molecular Dynamics,* in *Proceedings of 1985 Varenna School on MD Simulation of Statistical Mechanical Systems,* edited by G. Ciccotti and W. G. Hoover (North-Holland, Amsterdam, in press).
[7]G. Ciccotti and G. V. Paolini (unpublished).
[8]J. P. Hansen and I. R. McDonald, *Theory of Simple Liquids* (Academic, London, 1976).
[9]L. Verlet, Phys. Rev. **159**, 98 (1967).